Journal Pre-proofs

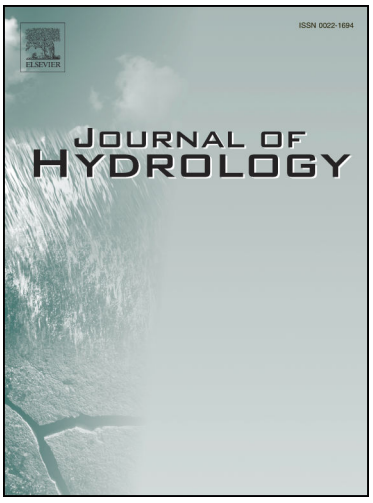

Hydrological characteristics of Australia: Relationship between surface flow, climate and intrinsic catchment properties

Jasmine B.D. Jaffrés, Ben Cuff, Chris Cuff, Iain Faichney, Matthew Knott, Cecily Rasmussen

PII: S0022-1694(21)00961-6
DOI: https://doi.org/10.1016/j.jhydrol.2021.126911
Reference: HYDROL 126911

To appear in: *Journal of Hydrology*

Received Date: 22 April 2021
Revised Date: 20 August 2021
Accepted Date: 1 September 2021

Please cite this article as: Jaffrés, J.B.D., Cuff, B., Cuff, C., Faichney, I., Knott, M., Rasmussen, C., Hydrological characteristics of Australia: Relationship between surface flow, climate and intrinsic catchment properties, *Journal of Hydrology* (2021), doi: https://doi.org/10.1016/j.jhydrol.2021.126911

Hydrological characteristics of Australia: relationship between surface flow, climate and intrinsic catchment properties

Jasmine B. D. Jaffrés[1], Ben Cuff, Chris Cuff, Iain Faichney, Matthew Knott, Cecily Rasmussen

C&R Consulting, 188 Ross River Rd, Townsville Qld 4814, Australia

[1]Jasmine@candrconsulting.com.au

Abstract

Streamflow and baseflow dynamics are driven by complex, interconnected catchment properties. A national study was conducted to assess the relationship between surface flow, climate and intrinsic catchment attributes in Australia. Subcatchments were delineated based on Horton's 5th stream order and were characterised by identifying parameters that influence streamflow and flood behaviour. Because observational datasets like rainfall and streamflow commonly have a non-normal distribution, the method of *L*-moments was applied to several time series. Surface hydrology and baseflow patterns were represented by twenty indices, which were statistically summarised via principal component (PC) analysis, yielding six PCs. Forty catchment descriptors from the themes of climate, topography, surface condition and hydrogeology were used to investigate their link with runoff patterns. Among these is the land surface value, a newly defined index incorporating soil properties and land use to estimate the capacity for water infiltration. Each metric was explored via correlation and regression analysis against the surface hydrology PCs and their influence on runoff discussed. The predictive skill of the regression models is improved when non-perennial waterways are excluded. Although rainfall characteristics dominate streamflow behaviour, topographical and surface conditions also greatly impact on runoff, especially during low-flow periods.

Keywords: Climate variability; Non-perennial streams; Surface hydrology; Topography; Soil field capacity; Water infiltration

1 Introduction

Streamflow behaviour and associated flood risk are influenced by a multitude of competing factors, both extrinsic (e.g. climate) and intrinsic (e.g. geology, soil, topography, land use and size). On a global scale, Beck et al. (2015) indicated that climate-related variables exhibited the strongest links to streamflow properties. Conversely, finer-scale studies suggested more nuanced links, highlighting the influence of soils (Trancoso et al., 2017; Zimmer and Gannon, 2018) and topography (Karlsen et al., 2019). Further, although precipitation patterns dominate high-flow events, Carlier et al. (2018) demonstrated the importance of geology in attenuating flow volumes by modifying subsurface water storage and consequently the flow duration curve, ultimately also affecting baseflow properties. Similarly, Lacey and Grayson (1998) determined a strong link between baseflow and both geology and vegetation, whereas topographical features were deemed irrelevant. Despite the complex influence of inherent catchment attributes on low flows, climate-associated characteristics such as rainfall and humidity still tend to explain a large proportion of baseflow variability and recession (Peña-Arancibia et al., 2010; van Dijk, 2010). Saft et al. (2016), in turn, emphasised that the partitioning of rainfall-runoff does not remain stationary, with the proportional runoff decreasing during drought periods.

Catchments can be characterised by wide-ranging combinations of attributes. Stein et al. (2009) analysed Australia's stream network based on 48 ecohydrological traits, ranging from climate, water balance, topography, substrate and vegetation. Kennard et al. (2010b) investigated 120 ecologically relevant metrics to assess flow regime types in Australia. Trancoso et al. (2017) explored 24 diverse biophysical properties to streamflow signatures in eastern Australia, emphasising the importance of soils on a regional scale. In a regional study of three tropical catchments in northern Australia, Erskine et al. (2017) focussed on geomorphological attributes to classify rivers in subcatchments. A New Zealand article

categorised rivers according to climate, topography, geology and land cover characteristics (Snelder and Biggs, 2002). In Europe, Kuentz et al. (2017) compared 16 flow signatures with 35 catchment descriptors, identifying the primary importance of geology for baseflow and the controlling influence of topography on streamflow flashiness.

Whereas countries like New Zealand (Snelder and Booker, 2013) and the United Kingdom (National River Flow Archive; Dixon et al., 2013) have relatively dense and more evenly distributed stream gauge networks, Australia's vast, dry interior is scarcely monitored. Similarly, rainfall data availability in Australia is significantly biased towards populated regions, with much higher observational network densities in the coastal southwest and south-eastern regions of the country (Jaffrés et al., 2018). Variables with poor translational properties, including catchment-specific streamflow characteristics, cannot be meaningfully applied to neighbouring drainage basins without extensive knowledge of relevant factors impacting on the attribute. For instance, rain shadows can produce vastly dissimilar runoff properties in two neighbouring catchments, potentially compounded by differing geology and land surface features. Hence, for large, nationwide studies of streamflow traits, reliance on alternative datasets is required. Albeit individually not fully representative of streamflow dynamics, these datasets can, in combination, provide information about flow characteristics and associated exposure to extreme flow events.

The overarching aim of this study is to assess whether a set of catchment descriptors are sufficiently representative of surface flow characteristics to warrant their use in ungauged sites. To fulfil this objective, the subsidiary aims of this article entail:

1) the derivation of forty metrics for every subcatchment throughout mainland Australia and Tasmania, covering the themes of climate, topography, land surface condition and hydrogeology; and

2) to analyse their relationship with twenty streamflow variables – ranging from baseflow attributes to high-flow properties – at unregulated stream gauge sites across Australia.

A description of each of the core datasets and any transposition or processing of data used is presented in section 2. The statistical results are summarised in section 3, whereas the relationship with aggregated streamflow properties is discussed in detail in section 4. Several recommended avenues for future research are offered with the conclusions (section 5). A more detailed explanation of statistical methods (appendix A) and soil classification (appendix B) is provided in the supplementary file.

2 Methods

In the Australian landscape, land use, soil characteristics and permeability strongly influence overland flow and are therefore included in this analysis. For this study, Australian subcatchments were summarised by forty variables. The parameters chosen cover five themes: climate, topography, surface condition, hydrogeology and surface hydrology. Each theme comprises several variables obtained from processing one or more datasets. In contrast to some other studies (e.g. Merz and Blöschl, 2005; Wagener et al., 2004), metrics of geographic proximity were not considered. This exclusion was rationalised to avoid unwarranted bias of similarity derived solely from proximity. Many Australian catchments are ungauged, especially in more remote regions. Therefore, hydrological data were used independently to determine the relevance of selected catchment properties to streamflow response in ungauged drainage basins.

Conventional use of statistical parameters on climate and hydrological datasets is confounded by their non-normal distribution. The method of *L*-moments describes the shape of a probability distribution without assuming normality (Hosking and Wallis, 2005). *L*-

moments were developed as a form of distributional analysis specifically for hydrological analysis (Castellarin et al., 2012). *L*-moments provide a more realistic estimation of extreme values from climate and hydrological data more typical of the Australian setting where extreme events in non-normal data distributions are common (Rahman et al., 2012). Consequently, *L*-moments (Hosking and Wallis, 2005) were derived to summarise these data, including rainfall, evaporation, mean sea level pressure (MSLP) and streamflow variables. For *L*-moments $l_{r\geq3}$ (where *r* is the moment of interest), *L*-moment ratios ($\tau_r = l_r/l_2$) were also calculated. A detailed description of the derivation method is available in appendix A.1. *L*-moments are analogous to mean (l_1), standard deviation (SD; l_2), skewness (τ_3) and kurtosis (τ_4) and super-skewness (τ_5). Henceforth, *L*-moment ratios τ_3 to τ_5 are also referred to as *L*-moments for simplicity.

2.1 Surface hydrology

Streamflow data from hydrological stations were incorporated to investigate the relationship between the catchment variables and flow characteristics. Average daily flow volumes from the Australian network of 4676 stream gauges were downloaded from Bureau of Meteorology (BoM) Water Data Online (WDO; http://www.bom.gov.au/waterdata/) website in July 2018. The network is heavily weighted towards well-defined river networks. In contrast, some large regions with low annual rainfall totals (e.g. the Nullarbor Plain and central Australia) have little to no data, possibly owing to the perceived low-risk of flooding to people and infrastructure. Further, the WDO database does not contain all stations publicly available from the relevant regional department. Eighteen stations from the Northern Territory were missing from the WDO database at the time of data download, even though those time series were available on the regional website (https://nt.gov.au/environment/water/water-information-systems/water-data-portal).

The quality of stream gauge data is highly varied and is dependent on numerous factors. For the purpose of this study, stations with long, reliable data records that are minimally impacted by anthropogenic changes were targeted. The BoM has compiled two lists of stations deemed

of superior quality: The list of BoM hydrologic reference stations (HRS; 31 August 2020 version; http://www.bom.gov.au/water/hrs/) catalogues 467 stations with long data record (≥ 30 years), located in unregulated catchments that underwent minimal land use change. Of these stations, 460 are accessible from WDO (Table 1). A second, more extensive register was compiled by the BoM for modelling purposes to identify gauges with high-quality data that cover at least ten years (Zhang et al., 2013). Similarly to the HRS, selected sites were also characterised as unregulated and unimpaired (limited irrigation and non-intensive land use). This dataset is henceforth referred to as the unregulated modelling stations (UMS). Of the 786 UMS listed, 714 were accessible from WDO (Table 1).

In total, 397 stations are contained in both HRS and the UMS datasets. A further 380 stations were contained only in HRS or the UMS, amounting to 777 stream gauges deemed of good quality. WDO stations were removed if the length of their record was less than fifteen years long or if they never recorded any flow. Records shorter than fifteen years are unlikely to include a large rainfall event, significantly underestimating the potential for flooding (Kennard et al., 2010a). Although more extensive time series are preferable to capture streamflow variability over longer timescales, the application of a more stringent threshold would further reduce the already limited spatial spread of the dataset because of the relative brevity of historic data records at many sites. Of the 777 HRS and UMS gauges, 27 had less than 15 years of available data and were thus omitted from further analysis. The remaining river gauging stations (n = 750) were used in this study (Figure 1) to derive twenty surface hydrology variables.

Table 1: Number of streamflow stations available from WDO per criteria.

Source	Criteria	Number of accessible stations (WDO)
WDO	tabulated in WDO (n = 6518)	4676
WDO	≥ 15 years of data in WDO	2821
WDO and HRS	tabulated as HRS (n = 467)	460
WDO and UMS	tabulated as UMS (n = 786)	714
WDO and HRS / UMS	≥ 15 years of data and listed as HRS and/or UMS	750*

*One station is situated on an island (A5130501, Kangaroo Island). Thus, that site does not have a corresponding match in the extracted subcatchments, because these are limited to mainland Australia and Tasmania (i.e. WDO n = 749).

Figure 1: Distribution of unregulated, WDO-derived stream gauges in Australia with a minimum data record of 15 years. The colour scheme distinguishes non-perennial and permanent streams. Borders of states and territories are also shown.

Surface flow data were summarised by considering data distributions for different regions across Australia. For example, flow data in Queensland (Figure 1) are typically characterised by high-flow (including flood) events, followed by extended periods with little to zero flows. Conversely, Victoria has consistent flows for most of the year, with only occasional peaks in flow. Consequently, a flow "peak" was defined as any event with a flow rate above the 80th percentile. In Australia, non-perennial streams are widespread, with flows ceasing at times in approximately 70% of river channels (Busch et al., 2020; Vidal-Abarca et al., 2020). Many of these seasonally dry, non-perennial streams are classified as intermittent waterways, fed by groundwater that permits more prolonged flows. Other non-perennial channels are more ephemeral in nature, only flowing briefly in direct and fast response to precipitation – without connectivity to groundwater (Busch et al., 2020; Vidal-Abarca et al., 2020). Because of highly sporadic flow at many gauged sites, twenty stations with a minimum record of 15 years returned 80th percentiles of 0 ML/Day. Hence, every flow event contributed a flow peak for those stations. For two peaks to be considered separate events, the flow had to return to below the 80th percentile (or to no-flow). If multiple peaks were registered within a 6-day window, only the main peak was selected.

Maximum and minimum recorded flow, average peak value and average number of peaks in a year are among the variables derived from the hydrological data. The 1st to 5th *L*-moments of daily flow were also extracted. The 5th *L*-moment, super-skewness, is potentially relevant in instances of extreme skewness. For example, in some regions of Queensland, many streams are without flows for most of the year, and this pattern may be more noticeable in

the 5th *L*-moment. The logarithmic $\log_{10}(x + 1)$ forms were also produced for variables with positively skewed distribution (with the exception of 3rd to 5th *L*-moments). This equates to a total of twenty indices for surface hydrology (Table 2).

Table 2: Surface hydrology and baseflow variables.

Variable		Unit	Description
Surface Hydrology	maximum surface flow	m^3/s	highest observed flow volume
	minimum surface flow	m^3/s	lowest observed flow volume
	average peak flow	m^3/s	mean of peak flows during high-flow events
	flow peaks per year		number of annual flow peaks
	surface flow *L*-moment 1	m^3/s	mean flow
	surface flow *L*-moment 2	m^3/s	standard deviation of flow
	surface flow *L*-moment 3	m^3/s	skewness of streamflow
	surface flow *L*-moment 4	m^3/s	kurtosis of streamflow
	surface flow *L*-moment 5	m^3/s	super-skewness of streamflow
	log maximum surface flow	m^3/s	logarithm of highest observed flow volume
	log minimum surface flow	m^3/s	logarithm of lowest observed flow volumes
	log average peak flow	m^3/s	logarithm of mean of peak flows during high-flow events
	log number of flow peaks		logarithm of number of annual flow peaks
	log surface flow *L*-moment 1	m^3/s	logarithm of mean flow
	log surface flow *L*-moment 2	m^3/s	logarithm of flow variability
BFI	baseflow index (BFI)		index of delayed shallow subsurface flow
	summer BFI		average BFI during summer (Nov–Apr)
	winter BFI		average BFI during winter (May–Oct)
	ratio of winter to summer BFI		ratio of average summer to average winter BFI
	log ratio of winter to summer BFI		logarithm of ratio of average summer to average winter BFI

2.2 Hydrogeology

This study used two hydrogeological types of variables as numerical inputs. The first, the dimensionless baseflow index (BFI), describes streamflow properties during low-flow periods, providing an estimate of water security. The second, subsurface permeability, measures how well subsurface rocks within a catchment transmit water. These two indices were chosen for their importance in controlling catchment flow behaviour and the relevance of the data obtainable from national datasets. The inconsistency of data availability throughout Australia restricted the use of other hydrogeology signatures (e.g. seasonal water table fluctuation, depth to water table, or seasonal lag response to rainfall).

2.2.1 Baseflow index (BFI)

Baseflow is long-term discharge to the river from natural storages including groundwater, soil moisture or bank storage (Hill et al., 2013). Baseflow is best defined as the component of streamflow that is not allocated to quickflow (e.g. overland runoff, interflow and direct precipitation). The BFI is the ratio of baseflow volume to total streamflow volume for a specified time period. Groundwater typically contributes the largest volume to baseflow. BFI is therefore an indicator of stream reliance on groundwater input.

Baseflow is recognised as an important component of the total flood hydrograph, particularly in areas of high BFI and for smaller or frequent flood events (Hill et al., 2013). This is especially applicable when catchments contain aquifers with high yield (Brown et al., 2011).

Many methods for BFI derivation exist, most of which involve analyses of hydrographs to separate the baseflow component. For Project 7 of the updated Australian Rainfall and Runoff guidelines, methods were developed to estimate BFI values for ungauged catchments from catchment characteristics such as geological conditions, soil type, climate and topography (Brown et al., 2011; Murphy et al., 2011). Those characteristics are used independently in the multivariate analysis of this study. Therefore, the BFI is calculated from the hydrographs available (streamflow data, section 2.1). Recursive digital filters are among the commonly applied approaches to derive baseflow characteristics (Singh et al., 2019; Su et al., 2016), including the low-pass filtering technique by Lyne and Hollick (1979). Their popularity at least partially stems from their ease of automation and the reproducibility of results. However, the pertinence of the Lyne-Hollick method is regionally dependent and may also vary for individual events (Kinkela and Pearce, 2014).

Quickflow and baseflow components of streamflow were separated from hydrograph data by applying the recursive digital filter method (Lyne and Hollick, 1979):

$$f_k = af_{k-1} + \frac{1+a}{2}(y_k - y_{k-1}) \quad , y_k \geq f_k \geq 0$$

where f_k is the filtered quick response at the k^{th} sampling instant, y_k is the original streamflow, a is the filter parameter and $y_k - f_k$ is the filtered baseflow. A filter value (a) of 0.98 was adopted, following the recommendation by the Commonwealth Scientific and Industrial Research Organisation (CSIRO) and SKM (2010). The filter was applied to the streamflow data three times: 1) forward pass filtering (y_k = original streamflow; initial quickflow, f_1, set to zero), 2) reverse pass filtering to nullify any phase distortion of the data because of the forward pass of the filter (y_k = filtered baseflow derived in step 1) and 3) forward pass filtering for further flow separation (y_k = filtered baseflow calculated in step 2) (Lyne and Hollick, 1979). Short streamflow data gaps (≤ 7 days) were filled via linear interpolation. Longer gaps were treated as breaks in the data. Unbroken interpolated streamflow records covering a minimum period of four years were individually utilised to derive baseflow estimates for each gauging site. The BFI for that stream gauge was then obtained by dividing the combined total baseflow of all these periods by the corresponding total streamflow (Figure 2a). To obtain seasonal indices, the baseflow estimates were split into summer (November to April; Figure 2c) and winter (May to October; Figure 2d) periods, with BFIs derived by dividing the relevant seasonal total baseflow by the analogous total streamflow. The ratio of the two seasonal BFIs (ratio of winter to summer BF; Singh et al., 2019) was also calculated (Figure 2b). The distribution of the resulting BFI ratios was distinctly right-skewed. Therefore, the logarithmic form was extracted as well. A total of 3691 stream gauges had sufficiently long, uninterrupted flow records to derive the BFI variables. The BFI was included in the surface hydrology analysis (Table 2) to determine subcatchment predictors significantly correlated with streamflow dynamics.

Regulated releases make river levels artificially higher in the dry months. The calculation of baseflow indices in regulated rivers is thus problematic, with BFIs for such streams overestimating baseflow. The BFI may be computed from data spanning as little as two years (Meyboom, 1961), but if results are intended as direct inputs for rainfall-runoff or flood models, ten years of data or more are recommended (Hill et al., 2013). For hydrological

studies such as this, it is preferable to include as many sites as feasible to maximise catchment characterisation without compromising the quality of the variables.

Figure 2

2.2.2 Subsurface permeability

Permeability (k [m^2]) is a property of soils, rocks and sediments. The attribute describes how quickly water flows into or through an aquifer or aquitard and the volume of such flux. This study focused on permeability of near-surface aquifers rather than hydraulic conductivity, because the latter can be derived from the former.

Permeability allocation was obtained from the Australian Hydrological Geospatial Fabric (AHGF or Geofabric; http://www.bom.gov.au/water/geofabric/index.shtml) groundwater cartography product v2.1.1. This database contains the greatest detail for the Australian continent (cf. global datasets of Dürr et al., 2005; Hartmann and Moosdorf, 2012). The Geofabric contains a map of surface hydrogeological units based on the 1:1,000,000 scale surface geology map (Geoscience Australia, 2012). These units fall within the categories (hydrogeological complexes, n_{max} = 48) defined in the National Aquifer Framework (NAF; http://www.bom.gov.au/water/groundwater/naf). Table 3 shows a list of relevant complexes. Surface lithology most commonly reflects subsurface lithology at shallow depth. Hence, it is assumed that the surface lithology is representative of the shallow subsurface (<50 m). However, subsurface permeability is often very heterogeneous in nature and reliable estimates are difficult to obtain, even for individual subcatchments (Calver, 2001; Shanafield and Cook, 2014).

Table 3: Geofabric lithologies and correlated regional saturated permeability groups (from Gleeson et al., 2011).

Geofabric code (IAF)	Lithologies from Australian Hydrological Geospatial Fabric (hydrogeological complexes)	k_s group number (refer to Table 4)
1	Surficial sediment aquifer (porous media – unconsolidated)	3
2	Upper Tertiary/Quaternary aquifer (porous media – unconsolidated)	1
3	Upper Tertiary/Quaternary aquitard (porous media – unconsolidated)	2
4	Upper Tertiary aquifer (porous media – unconsolidated)	1
5	Upper Tertiary aquitard (porous media – unconsolidated)	2*
6	Upper mid-Tertiary aquifer (porous media – unconsolidated)	1
7	Upper mid-Tertiary aquitard (porous media – unconsolidated)	2
8	Lower mid-Tertiary aquifer (porous media – unconsolidated)	1
9	Lower mid-Tertiary aquitard (porous media – unconsolidated)	2
10	Lower Tertiary aquifer (porous media – unconsolidated)	1
11	Tertiary basalt aquifer (fractured rock)	8
12	Tertiary sediments (fractured rock)	4
13	Mesozoic sediment aquifer (porous media – consolidated)	5
14	Mesozoic fractured rock aquifers	7
15	Jurassic (Great Artesian Basin (GAB) intake beds) (porous media – consolidated)	5
16	Mesozoic (GAB) (porous media – consolidated)	5
17	Fractured and karstic rocks, local aquifers	6
18	Fractured and karstic rocks, regional-scale aquifers	6
19	Palaeozoic and Precambrian fractured rock aquifers (low permeability)	4
20	Palaeozoic and Precambrian fractured rock aquifers (consolidated and partly porous)	7
21	Late Permian/Triassic intrusives and volcanics fractured rock aquifers	8
22	Late Permian/Triassic sediments (porous media – consolidated)	5
23	Palaeozoic and Precambrian fractured rock aquifers (low fracture density and very low permeability)	4
25	Water body	Not used

*In Geofabric, these data are part of IAF code 1 (k_s group number 3).

Surface lithology types were then allocated a permeability category (Table 3 and Table 4). Gleeson et al. (2011) collated 230 regional saturated permeability (k_s) values from global calibrated groundwater models (predominantly from North America; none from Australia) to produce averages for generalised hydrolithology groups (Table 4). The mean permeability values are expressed as logarithmic permeability (log k_s) in Table 4 and represent saturated permeability at a regional scale (>5 km).

Table 4: Hydrolithology groups and permeability, k_s [m^2] (modified from Table 1 in Gleeson et al., 2011).

k_s group number	Log k_s [log(m^2)]	Description
1	-10.9	Coarse grain unconsolidated
2	-14.0	Fine grain unconsolidated
3	-13.0	Undifferentiated unconsolidated
4	-16.5	Fine grain siliciclastic sedimentary
5	-15.2	Undifferentiated siliciclastic sedimentary
6	-11.8	Carbonate
7	-14.1	Crystalline
8	-12.5	Volcanic

For this study, the hydrogeological complexes of the Geofabric were allocated a k_s value according to their lithological descriptions (refer to k_s group numbers, Table 3 and Table 4). For example, both "Upper Tertiary/Quaternary Aquifer (porous media - unconsolidated)" and "Lower Tertiary Aquifer (porous media - unconsolidated)" are allocated as k_s Group 1 (coarse grain unconsolidated) because they are termed aquifers as opposed to aquitards, denoting higher permeability and unconsolidated sediment.

2.3 Topography and subcatchment delineation

The continent-scale National River Basin Boundary (NRBB) dataset (Geoscience Australia, 1997), based on topographical and hydrological interpretation, provides a commonly adopted definition of 233 river basins (catchments) across mainland Australia and Tasmania. However, the spatial scale of these river basins is too coarse to be sensitive to the full range of flood-related parameters used in this study. Therefore, the river basins of the NRBB dataset were further divided into subcatchments based on the Horton (1945) 5^{th}-order stream definition and the National Topographic Vector Database (Geoscience Australia, 2006), resulting in subcatchments large enough to enable meaningful comparisons and small enough to allow for computing power and timeframe constraints. The upstream area of 6^{th} and higher-order waterways (i.e. downstream subcatchments) does account for upstream subcatchment areas.

The NRBB dataset was used as the primary layer to clip both the topographical vector database (Geoscience Australia, 2006) and the digital elevation model (DEM; Geoscience

Australia, 2011) into 233 separate basins via the ArcGIS software (v9.3.1). An external buffer zone of 10 km was applied to each river basin when clipping the DEM to ensure reliable identification of the catchment margin. The buffer zone was specifically required because the NRBB dataset is not based on the DEM, with the applied basin boundaries therefore not necessarily agreeing with the elevation data. The centroid of each river basin was used to determine its appropriate Map Grid of Australia (MGA) zone (zones 50 to 56). The basin data, including DEMs (Geoscience Australia, 2011), were then projected into their relevant MGA zone.

The GIS-based software package CatchmentSIM (version 3.0.3.1) was employed to divide the river basins into subcatchments on a Horton's 5th-order stream basis and a raster 3" DEM (Figure 3). This involved the generation of streams within the software from stream initiation points derived from the existing mapped stream networks. The CatchmentSIM catchment breakup approach used a Horton stream ordering algorithm, which delineates subcatchments of a particular Horton order based on the vector stream network. Every segment of 6th- and higher-order streams is defined as a separate subcatchment. However, if multiple 5th- and higher-order streams entered the ocean within the same NRBB-defined catchment, these were treated as the same subcatchment by the software (Figure 3c). In total, 2816 subcatchments were obtained.

Figure 3

In addition to the delineation of the river basin subcatchments, CatchmentSIM was also used to calculate topographical variables for each subcatchment. These derived datasets were reprojected from their MGA zone to a geographic coordinate system, the Geocentric Datum of Australia 1994 (GDA94), to enable merging into a single coherent national dataset. In total,

eighteen CatchmentSIM indices were utilised in this study (cf. topography predictors in Table 5).

Table 5: The forty descriptors investigated for their link to surface hydrology (HG = hydrogeology; SD = standard deviation).

Variable		Unit	Description
Climate	average number of rain days	days	average rainy days per year
	rainfall percentage in summer season	%	% rain that falls in Nov–Apr
	daily rainfall *L*-moment 1	mm	mean daily (rain day) rainfall
	daily rainfall *L*-moment 2	mm	SD of daily (rain day) rainfall
	daily rainfall *L*-moment 3	mm	skewness daily (rain day) rainfall
	daily rainfall *L*-moment 4	mm	kurtosis daily (rain day) rainfall
	summer season evaporation *L*-moment 1	mm	mean daily evaporation (Nov–Apr)
	summer season evaporation *L*-moment 2	mm	SD of daily evaporation (Nov–Apr)
	summer season evaporation *L*-moment 3	mm	skewness daily evaporation (Nov–Apr)
	winter season evaporation *L*-moment 1	mm	mean daily evaporation (May–Oct)
	winter season evaporation *L*-moment 2	mm	SD of daily evaporation (May–Oct)
	winter season evaporation *L*-moment 3	mm	skewness daily evaporation (May–Oct)
	summer season MSLP *L*-moment 1	hPa	mean daily MSLP (Nov–Apr)
	summer season MSLP *L*-moment 2	hPa	SD of daily MSLP (Nov–Apr)
	summer season MSLP *L*-moment 3	hPa	skewness daily MSLP (Nov–Apr)
	winter season MSLP *L*-moment 1	hPa	mean daily MSLP (May–Oct)
	winter season MSLP *L*-moment 2	hPa	SD of daily MSLP (May–Oct)
	winter season MSLP *L*-moment 3	hPa	skewness daily MSLP (May–Oct)
Topography	area	m^2	subcatchment area
	total upstream area	m^2	subcatchment area plus area of all upstream subcatchments
	slope	°	average subcatchment slope
	hill slope	°	average slope in hilly areas
	Horton's drainage density (HDD)		subcatchment stream density
	bifurcation ratio		high value: large proportion of 1^{st}-order streams low value: small proportion of 1^{st}-order streams
	main stream length	m	length of main flow path
	main stream slope	°	average slope of main flow path
	longest flow path length	m	length of longest flow path
	longest flow path slope	°	average slope of longest flow path
	average flow length	m	average flow path length in subcatchment
	flow length SD	m	SD of flow path length in subcatchment
	channel skewness		high value - asymetrical drainage pattern low value - symetrical drainage pattern

	maximum elevation	m	maximum elevation in subcatchment
	elevation range	m	elevation variation in subcatchment
	mean elevation	m	mean elevation in subcatchment
	median elevation	m	median elevation in subcatchment
	elevation SD	m	SD of elevation in subcatchment
LSV	land surface value		high value – high runoff low value – high absorbance
	land surface value SD		variability of land surface values
HG	average subsurface permeability	log(m^2)	measure of subcatchment's ability to transmit water underground
	subsurface permeability SD	log(m^2)	variability of subsurface permeability

Basin boundaries of the nationally defined river basin dataset (Geoscience Australia, 1997) provided the initial spatial division for the analysis. In some instances (e.g. the Murray-Darling river basin), the defined river basins flow from one into another within a larger drainage network. Stream orders are reset within each river basin, despite channels being part of a continuing larger drainage network. This resetting affects determination of the bifurcation ratio in larger catchments incorporating multiple basins, because a large watercourse will be re-assigned a stream order of 1 when flowing between basins. This effect highlights a limitation of using river basins to define the spatial areas for a nation-wide study. Likewise, the river basin boundaries in the Geoscience Australia (1997) dataset can adversely impact calculation of total upstream area for each subcatchment, when these river basins are part of a larger drainage network. Hence, the total upstream area may be underestimated. For the Murray-Darling River system, CatchmentSIM-derived upstream areas of affected subcatchments were manually adjusted to include relevant areas from adjacent basins.

CatchmentSIM identifies main channel flow while ignoring braided and anabranching channels. Therefore, Horton's drainage density (HDD), a measure of the total stream channel length per unit area, may be underestimated in low-gradient catchments

2.4 Climate

Rainfall data are available across Australia, with the BoM weather station network consisting of over 17,700 sites. All rainfall station records were accessed directly from BoM's Climate

Data Online (CDO; http://www.bom.gov.au/climate/data/) website in October 2017. By default, the CDO database only includes data that are deemed of acceptable quality – or were not yet quality-checked.

Once downloaded, multi-day rainfall totals covering a 2- to 4-day period were transformed into a daily average over the relevant period. Conversely, multi-day rainfall values over 5-day or longer periods were removed to reduce a potential positive bias in annual rain days. Rainfall stations with at least 30 years of data (n = 8539, Figure 4a) were used to extract six variables for this study (Table 5). Two of these indices required the additional stipulation of a minimum of thirty years with near-complete (>350 days of) yearly rainfall records at individual stations, reducing the data subset to n = 7880.

Figure 4

Rainfall has a distinct, non-uniform seasonal pattern in many Australian regions. For instance, winter rainfall is prevalent in the southwest and Tasmania. Conversely, in most parts of the country (including northern Australia and the eastern coast of the mainland) rainfall is summer-dominant. Australia's tropical regions are characterised by a summer wet season, defined by the BoM as November to April. This period was applied to define a rainfall seasonality variable. Rainfall for the period November to April was divided by the total yearly rainfall to obtain *rainfall percentage in summer season*. The index *average number of rain days* is defined as any day with a minimum precipitation of 0.2 mm. Both predictors were calculated from data of years with near-complete records (>350 days with data).

Australian rainfall data are characterised by a large number of days without rainfall and a right-hand skew representing several extreme events. Four variables were derived by

applying the method of *L*-moments based on the reduced rainfall dataset (rain days only). For each rainfall station, the first four *L*-moments were computed.

The BoM network of stations with evaporation (n = 632) or MSLP (n = 930) data is significantly smaller than the rainfall dataset (Figure 4). After removal of records flagged by the BoM's internal quality control, the remaining values were used if the station record exceeded two years (n = 532 for evaporation and n = 799 for MSLP, Figure 4b-c). The evaporation and MSLP data were split into summer (November – April) and winter seasons (May – October). The first three *L*-moments were then applied to both seasons separately, producing six descriptors for both evaporation and MSLP (Table 5).

Values for each of the eighteen climate variables were assigned to individual subcatchments in a multi-step process: For every subcatchments with relevant station measurements, each climate statistic within the polygon was averaged to assign a single value to that subcatchment. A radial basis function interpolation was applied using ArcGIS v10.4 to allocate values to catchments without climate stations.

2.5 Surface condition

The surface effect of either absorbing or repelling water is the greatest impact soil, geology and land use have on catchment response to rainfall. The term 'surface condition' is used to incorporate the key variables of soil, geology and land use influencing flood response. To determine a numerical value useful in later statistical analysis, a method representative of Australian surface conditions (or the relative surface state between absorbent and repellent) was developed. The diverse soil descriptions were aggregated into a simple, relative-rank land surface value (LSV), incorporating key parameters such as permeability (texture) and absorbance (clay content and behaviour), depth of soil profile (incorporating geological outcrop) and anthropogenic land use effects (Figure 5). The simplicity of this ranking approach, in contrast to detailed soil description, aligns with the Australia-wide resolution of catchment-response analysis for this study.

Figure 5

To calculate LSVs, national soils and geology data were first assessed to allocate a field capacity score (FCS) based on soil classification, depth and texture (Figure 5). Field capacity is defined as the maximum bulk water content retained in soil at −33 J/kg of hydraulic head (Veihmeyer and Hendrickson, 1931). More generally, the term is used to indicate the volume of stored water within a soil profile necessary to initiate permanent surface pooling or runoff. This measurement is an indication of the potential for soil to absorb water. Low field capacity reflects limited ability to absorb water, whereas high field capacity suggests the reverse. Field capacity is controlled largely by soil texture and composition and these characteristics are accounted for in the soil classification, depth of soil profile and texture ranks as described in the Australian Soil Classification (ASC; Ashton and McKenzie, 2001; Figure 3). More detailed description of field capacity score determination is provided in section 2.5.1.

Land use was characterised with a scoring range of -7 to +7. The land use score (LUS) was allocated on a scale from land use practices that improve or diminish soil field capacity. Section 2.5.2 outlines LUS determination in more detail. A final LSV was then assigned to the land surface based on the addition of field capacity and LUSs (section 2.5.3; Figure 6).

Figure 6

2.5.1 Field capacity score (FCS) determination

Soil and geology throughout Australia were assessed by evaluating the soil classification and distribution of CSIRO's Digital Atlas of Australian Soils (DAAS;

https://www.asris.csiro.au/themes/Atlas.html#Atlas_Digital). The soil codes of the atlas classification (~3000 soil descriptions) were converted into the ASC as per Ashton and McKenzie (2001), grouping the data into thirteen soil types (Figure 5).

Permeability and water holding property descriptions from widely used sources (Australian Soil Club; McKenzie et al., 2004; Victorian Resources Online) were utilised to conduct an initial assessment of soil field capacity to address the thirteen major soil groups. This evaluation assigned a rank score of 1 to 5 describing the permeability for the thirteen soil units by averaging the ranks used in the three available categorisation systems (Figure 5).

Assigning FCS on the basis of the ASC (Ashton and McKenzie, 2001) alone has its limitations. General descriptions do not consider factors such as the depth of the profile to bed rock, which in some instances may be minimal. To account for this, the descriptions in DAAS were reviewed to determine the depth to rock and the amount of rock outcrop within each mapped unit. For each map unit the soil profile was classified as Class A (rock outcrop - geology), Class B (rock outcrop/skeletal shallow soil cover over rock), Class C (rock outcrop/moderated soil cover over rock) or Class D (soil) (Figure 5). To define the overall FCS, further assessment of the soil texture was also required. DAAS descriptions give thirteen classes of soil texture. These were converted to a rank score of 1 to 7, assigned on the basis of textural classes from the existing classification, as per Charman (1978).

The three ranks derived from each of the three categories described earlier (i.e. soil classification, depth and texture) were combined into a three-point soil code with a sequential nomenclature. For example, a calcarasol with thick soil profile and calcareous earth texture would code 3D4. There are 676 possible permutations of code combinations but only 80 of these were identified across Australia. Hence, only these 80 codes or map units are used in further analysis (cf. Table B.1 for the full list of soil codes).

Allocation of FCS for each of the 80 codes was based on interpreting a significance weighting for each component of the soil code by applying *a priori* knowledge of their context,

composition and soil profile arrangement. For each soil code, the three ranked factors may have varying degrees of dominance, strong interactions or, in some instances, conflicting interactions. Therefore, the relative weighting of factors was considered for each individual code, resulting in nine characteristic weighting trends that formed the basis of FCS allocation (see appendix B2 for FCS allocation rationale). Final FCSs ranged from 1 to 7, with 1 representing high field capacity and 7 low field capacity.

2.5.2 Land use score (LUS) determination

National land use data (version 4, 2005-06) were obtained from the national Department of Agriculture Scale Land Use (https://www.agriculture.gov.au/abares/aclump/land-use/data-download). Detailed vector land use data for each state and territory (Figure 1) were merged into single coverage for the entire country. All land uses (Table B.3) were assigned a unique LUS value based on whether the land use would negatively affect field capacity (i.e. reduce field capacity: values 1 to 7), positively affect field capacity (i.e. increase field capacity: -1 to -7), or make no difference (0). A complete list of land use and allocated LUS is provided in appendix B3.

2.5.3 Land surface value (LSV) determination

Scores from the soil field capacity and the land use analyses were combined to allocate an LSV between -7 and +14 (Figure 6). This step reveals the impact of land use on field capacity as positive (low field capacity), negative (high field capacity) or neutral. There are several situations, however, when the end members of both soil/geology field capacity and land use may dominate the impact on absolute field capacity. Consequently, soil codes allocated an FCS of +7 (rocky areas excluding sandstones) or land use allotted an LUS of +7 (high-density urban and industrial areas) were assigned an LSV of +14. Conversely, land use allocated an LUS of -7 (water bodies such as dams and reservoirs) were assigned an LSV of -7 regardless of the FCS value.

2.6 Numerical methods

A principal component analysis (PCA) based on a correlation matrix and varimax rotation was performed on the twenty surface hydrology and BFI variables, reducing these to six surface hydrology principal components (PCs). The BFI was derived from surface water information, therefore reflecting streamflow conditions. Thus, the index was included with the surface hydrological data.

One stream gauge is situated on an island (A5130501, Kangaroo Island). This site was excluded from further statistical analyses because the subcatchment delineation is limited to mainland Australia and Tasmania. A correlation analysis based the Pearson correlation coefficient was performed between each subcatchment variable and the six surface hydrology PCs representing streamflow, with the aim of determining the relative significance of the relationship between these descriptors (cf. section 2 and appendix A). The correlation analysis may identify significantly related indices but is unable to determine whether there is a causal link between the two variables. Hence, a "false positive" (type I error) may occur, especially when the total number of compared indices is high. The Šidák correction factor, α_S (Šidák, 1967), was applied to reduce the false positive error rate:

$$\alpha_S = 1 - (1 - \alpha)^{1/n_p}$$

For n_p equal to forty catchment descriptors and significance level (α) of 0.05, a Šidák correction factor of 0.0013 is obtained. Thus, the correlation is deemed significant at the Šidák correction level if the p-value does not exceed 0.0013. The results provide context for the relative importance of each index in predicting streamflow dynamics.

A multiple linear regression analysis was conducted using software XLSTAT. Its linear regression tool permits the extraction of the best model per predictor number, along with associated criteria such as Bayesian information criterion (BIC), the Akaike's information criterion (AIC) and adjusted R^2 (R^2_{adj}). The BIC penalises overfitting more heavily than the

AIC, whereas the R^2_{adj} is most lenient. Henceforth, the XLSTAT output will be referred to as the best regression model (BRM) results.

An additional, more detailed regression analysis was then applied in MATLAB to explore all possible combinations with up to six input variables, similar to Saft et al. (2016). This computationally demanding method equates to 4.6 million regression models per PC. These 6_{max}-predictor regression models were then assessed using several criteria, including the adjusted R^2 (penalising for extra predictors), AIC, the AICc (correcting for small sample-size) and the BIC.

To evaluate the proportion of evidence for each predictor, the relative difference was calculated for the three criteria (AIC, AICc, BIC):

$$\Delta AIC_i = AIC_i - AIC_{min} ,$$

where AIC_{min} is the model with the lowest (best) AIC value and *i* refers to the ith model. The model weights (*w*) for each PC were then calculated as follows:

$$w_{i,\mathrm{PC}} = \frac{e^{\frac{-\Delta \mathrm{AIC}_{i,\mathrm{PC}}}{2}}}{\sum e^{\frac{-\Delta \mathrm{AIC}_{all,\mathrm{PC}}}{2}}} .$$

Finally, the combined total proportion of evidence (TPE) of every predictor (*p*) was obtained for each PC by adding all weights of models that contained the predictor:

$$\mathrm{TPE}_{p,\mathrm{PC}} = \sum w_{p,\mathrm{PC}}$$

A large proportion (76.7%) of the selected station network is located in non-perennial waterways and these sites therefore have a uniform low-flow of 0 m^3/s. Yet, these locations are characterised by diverse catchment properties, their link to streamflow potentially masked by their non-perennial status that are intermittent to ephemeral in nature (cf. Vidal-Abarca et al., 2020). Thus, the correlation and regression analyses were repeated for a subset (*n* = 175) that excludes all non-perennial systems.

3 Results

Six PCs summarise the twenty surface hydrology variables (Table A.2 and Figure A.1), accounting for a combined total of 91.4% of the variance. PC1 relates to the severity of extreme flow events. The probability of extreme flow events and baseflow attributes are characterised by PC2. The low-flow conditions are summarised with PC3, whereas the frequency of high-flow events is represented by PC4. PC5 explains the difference (ratio) between baseflow during summer and winter, whereas PC6 refers to general (seasonal and long-term) baseflow conditions. The correlation analysis between subcatchment variables and the six surface hydrology PCs (Figure 7) revealed distinct links between catchment characteristics and streamflow. These PC-specific connections are subsequently discussed in more detail.

Among the applied criteria, the BIC most heavily penalises overfitting. Thus, the smallest BRM sizes are consistently attributed to the BIC. The difference in selected predictor numbers between the various selection criteria (AIC, BIC and R^2_{adj}) is generally greater when the model strength is lower (i.e. lower R^2_{adj}). In addition, the increase in fitting performance tends to plateau after about four predictors for most PCs, comparable to the result by Saft et al. (2016). However, the fitting pattern is PC- and sample-dependent. For PC1, the predictive gain is reduced after the inclusion of the second variable when all streams are considered, whereas the perennial stream subset exhibits a strong preference for six predictors (in agreement with the BIC-selected BRM). Conversely, the fitting performance for PC2 suggests a relatively large predictor number (minimum of seven), regardless of whether non-perennial sites are excluded.

The 6_{max}-predictor regression models yielded comparable TPE results independently of the applied criterion (AIC, AICc or BIC). For the better-performing predictors, BIC (Figure A.2)

tends to have slightly lower TPE values. Subsequently, the lowest TPE result for individual predictors will be presented.

3.1 PC1

PC1 predominantly characterises extreme (maximum, mean peak and mean) flow conditions and flow variability (SD). Both the linear variables and their logarithmic counterparts are represented in PC1 (Figure A.1). This PC is more closely associated with climatic characteristics rather than intrinsic catchment properties. Fifteen (out of 18) climate metrics are significantly correlated with PC1 based on the more stringent Šidák correction factor (p-values < 0.0013), including all MSLP indices (Figure 7). Among the non-climatic predictors, variability of subsurface permeability and LSV, average LSV and main stream slope are the variables with the strongest association with PC1. The BRM test in XLSTAT returned linear equations of distinctly different size (*n*) dependent on whether the AIC (*n* = 25) or BIC (*n* = 8) were applied as the decisive criterion (Table 6). Their respective R^2_{adj} values are moderately high at 0.399 and 0.375. All predictors in the BIC model are also included in the more complex AIC selection. Among these are mean summer evaporation and MSLP, all winter MSLP characteristics, main stream slope and variability of subsurface permeability.

The greatest TPE for PC1 was obtained by variability of subsurface permeability (0.999), followed by mean summer MSLP (0.916_{AIC}), mean winter (0.470_{BIC}) and mean summer evaporation (0.380_{BIC}).

3.2 PC2

PC2 mainly embodies the probability of extreme flow events (*L*-moments 3-5) and, to a lesser extent, baseflow attributes. Similar to PC1, the list of predictors significantly correlated with PC2 is also dominated by climate variables (16 indices). Slope-related attributes (including slope of the main stream channel) are among significantly linked intrinsic catchment properties (p-values < 0.0013). Compared with the other PCs, the BRM provided the most

optimal results for PC2 in terms of both R^2_{adj} (0.600 and 0.596) and level of agreement between the AIC- and BIC-preferred output (*n* of 19 and 15, respectively; Table 6). Both AIC and BIC mostly incorporated climate metrics, including annual rainfall days, rainfall percentage in summer, all MSLP variables and most evaporation characteristics. In addition, variability of elevation and subsurface permeability are deemed significant predictors of PC2.

For PC2, six variables have TPE greater than 0.970 (variability of subsurface permeability, mean winter MSLP, MSLP variability in both seasons, the number of rain days and rainfall kurtosis), whereas the remainder have TPE below 0.030.

3.3 PC3

PC3, characterising low-flow conditions (represented by minimum flow), has the fewest number of predictors that are significantly correlated (p-values < 0.0013). These include slope, HDD, the bifurcation ratio and the number of annual rain days. The BRM indicates a relatively poor fit when a linear relationship between catchment characteristics and PC3 is assumed (Table 6). The BIC-preferred model size is four (R^2_{adj} = 0.122) whereas the AIC produces a much more complex output without notable gain in explanatory power (*n* = 28; R^2_{adj} = 0.167). The predictors in the BIC model are average slope, bifurcation ratio, main stream slope and annual rain days.

The TPE for PC3 are dominated by bifurcation ratio, average slope, main stream slope and annual rain days (all above 0.990), whereas HDD reached a TPE_{BIC} of 0.530.

3.4 PC4

A broad range of predictors is significantly linked to PC4, representative of the frequency of high-flow events (p-values < 0.0013). Twenty-eight catchment variables are significantly related to PC4 at the Šidák correction level (p-value < 0.0013; Figure A.1 and Table A.3). Notably absent from the 28 significant predictors are most rainfall indices (except for annual rain days). The R^2_{adj} values of the BRM were quite high for both the AIC (R^2_{adj} = 0.452; *n* =

29) and BIC (R^2_{adj} = 0.423; *n* = 15; Table 6). Stream density (HDD), LSV properties, annual rain days, rainfall skewness and various evaporation and MSLP features are among the significantly linked variables linked to PC4.

Variability of evaporation in both seasons and summer MSLP explained most of PC4 (TPE > 0.980), whereas HDD, LSV variability and rainfall kurtosis had TPE values ranging from 0.699 $_{BIC}$ to 0.752$_{BIC}$.

3.5 PC5

PC5 exemplifies the ratio of winter to summer BFI. Climate metrics are again the most prominent indices significantly associated with PC5 (p-values < 0.0013). Relevant non-climatic, intrinsic predictors are limited to elevation characteristics and variability of subsurface permeability. Along with PC2, the BRM fits were among the poorest of the six PCs (Table 6). In addition, both AIC (*n* = 12; R^2_{adj} = 0.143) and BIC (*n* = 4; R^2_{adj} = 0.127) produced the smallest model size compared to the other PCs. The BIC-preferred model incorporated variability of subsurface permeability, skewness of winter evaporation and summer MSLP, and mean winter MSLP.

For PC5, the skewness of winter evaporation (TPE of 0.837$_{BIC}$) is the most relevant predictor, followed by subsurface permeability (0.441$_{BIC}$) and mean winter MSLP (0.410$_{BIC}$).

3.6 PC6

Baseflow conditions are summarised by PC6. Twenty-nine predictors are significantly connected to PC6 (p-values < 0.0013), including a wide range of climatic and in-situ properties. The BRM analysis produced a moderate fit for both AIC (R^2_{adj} = 0.350; *n* = 28) and BIC (R^2_{adj} = 0.303; *n* = 5). BIC-relevant metrics are maximum elevation, LSV variability, annual rain days, rainfall kurtosis and MSLP variability in winter.

Annual rain days (0.989_{BIC}) and maximum elevation (0.892_{BIC}) have the highest TPE for PC6, with winter MSLP and LSV variability, summer rainfall proportion and rainfall kurtosis all having TPEs greater than 0.5.

Figure 7

Table 6: Best regression model results. The adjusted R^2 (model size) values of the model with the lowest AIC and BIC values per PC are listed.

Criterion	PC1	PC2	PC3	PC4	PC5	PC6
AIC	0.399 (25)	0.600 (19)	0.167 (28)	0.452 (29)	0.143 (12)	0.350 (28)
BIC	0.375 (8)	0.596 (15)	0.122 (4)	0.423 (15)	0.127 (4)	0.303 (5)

4 Discussion

Forty subcatchment-specific metrics were investigated for their connection to Australian streamflow properties that were summarised with six PCs. All examined catchment variables exhibited significant links to surface hydrology (Table 7). Rainfall attributes have an overwhelming influence on extreme flow events and their likelihood. Conversely, low-flow periods are more dependent on in situ conditions, including topographical features and subsurface permeability. These results are thus in close agreement with previous studies that explored controls of streamflow patterns (e.g. Kuentz et al., 2017).

Table 7: Results of correlation analysis between subcatchment variables and six surface hydrology principal components (SD = standard deviation).

Variable		Surface hydrology component affected	Interpreted descriptor impact on flow conditions
Topog	(subcatchment) area	high-flow probability; baseflow character	Greater catchment areas typically result in greater volumes of flow, supporting more extreme flows and increased baseflow.

Variable		Surface hydrology component affected	Interpreted descriptor impact on flow conditions
	total upstream area	low-flow character; flood probability and severity	Greater upstream areas typically result in greater volumes of flow, supporting more extreme flows and increased baseflow.
	slope	flood probability; low-flow character	Steeper slopes cause runoff to reach downstream regions faster.
	hill slope	high-flow frequency; baseflow	Hill slopes define the effects of upstream flows on the catchment and influence both high- and low-flow properties.
	Horton's drainage density (HDD)	high-flow frequency; low-flow conditions and baseflow	HDD is related to the capacity of a catchment to drain water downstream. Therefore, a greater HDD supports shorter-duration high-flow events, with rapid return to low flow.
	bifurcation ratio	low-flow character	Bifurcation, a measure of lower- and higher-order streams within a catchment, will cause less efficient flows at lower ratios.
	main stream length	baseflow, low-flow conditions; extreme flow severity	As longer streams are commonly attributed to larger catchment size, the likelihood of a catchment-wide rainfall event is reduced. In addition, longer exposure to evaporation reduces the surface water volume.
	main stream slope	low-flow conditions; flood severity	Steeper slopes encourage more rapid runoff.
	longest flow path length	baseflow; high-flow probability	As longer flow paths are commonly attributed to larger catchment size, the likelihood of a catchment-wide rainfall event is reduced. In addition, longer exposure to evaporation reduces the surface water volume.
	longest flow path slope	flood probability; baseflow	A steeper slope along the longest flow path suggests more rapid runoff.
	average flow length	flood probability	Similar to main stream length, the average flow length determines likelihood of catchment-wide rainfall event.
	flow length SD	baseflow; flood frequency	Flow length tends to vary more in subcatchments with little vertical relief, suggesting less efficient drainage in those basins.
	channel skewness	flood frequency	Channel skewness relates to the symmetry of a catchment, with higher skewness associated with less efficient flows into streams.
	maximum elevation	flood probability; baseflow	Higher maximum elevation tends to coincide with more frequent rain days in the elevated areas. Consequently, a greater number of flow peaks is commonly observed. Very high values of maximum elevation may suggest precipitation in the form of snowfall, encouraging runoff delay, which will adjust the peak conditions of flows.

Variable		Surface hydrology component affected	Interpreted descriptor impact on flow conditions
	vertical range	flood probability and frequency; baseflow	Similar to the effects of maximum elevation. A greater vertical range tends to encourage efficient runoff.
	mean elevation	flood frequency; baseflow	Subcatchments with higher elevation tend to have greater baseflow yield.
	median elevation	flood frequency; baseflow	Subcatchments with higher elevation tend to have greater baseflow yield.
	elevation SD	flood probability and frequency; baseflow	Similar to the effects of maximum elevation. A greater variability in elevation tends to encourage runoff.
LSV	LSV	flood frequency and baseflow	LSV affects the amount of runoff by influencing rainfall infiltration. Higher LSVs suggest a greater proportion of rainfall being retained by streams, encouraging more extreme flows.
	LSV SD	flood frequency; baseflow	More variable LSVs suggest a complex landscape with localised increased infiltration of water.
Permeability	mean subsurface permeability	baseflow	Subsurface permeability affects water loss and, thus, baseflow properties.
	subsurface permeability SD	flood severity and probability; baseflow seasonality	Similar to LSV SD, more varied subsurface permeability suggests a complex landscape with localised increased infiltration of water helping to reduce flow volumes.
Climate	number of rain days	flood probability and severity; high-flow frequency;low-flow conditions; baseflow	An increased number of rain days affects pre-wetting (soil saturation state), which can change runoff profiles. Elevated baseflow is also promoted.
	rainfall percentage in summer season	flood probability and severity; baseflow average and seasonality	A larger proportion of summer season rainfall increases the risk of flood events.
	rainfall (1st *L*-moment)	flood probability and severity; baseflowaverage and seasonality	Higher mean daily rainfall suggests an increased risk of flood events.
	rainfall (2nd *L*-moment)	flood probability and severity, baseflow average and seasonality	The variability of rainfall will dictate the nature of rainfall events within individual catchments, affecting both high- and low-flow signatures.
	daily rainfall (3rd *L*-moment)	flood probability and severity; baseflow	A highly skewed rainfall distribution is often a signal that the basin is prone to storm events and also produces positively skewed streamflow patterns.
	daily rainfall (4th *L*-moment)	flood probability; baseflow	Large positive kurtosis values indicate heavier tails. Hence, similar to skewness, this variable provides information about the probility of extreme rainfall events.
	evaporation in summer season (1st *L*-moment)	flood probability and severity; high-flow frequency; baseflow	Regions with higher evaporation will have significantly reduced runoff, because evaporation will reduce the available water. Lower evaporation rates are also indicative of wetter conditions.

Variable	Surface hydrology component affected	Interpreted descriptor impact on flow conditions
evaporation in summer season (2nd *L*-moment)	high-flow frequency	High evaporation variability suggests fluctuating evaporation rates (and, hence, sporadic cloud cover and rainfall), indicating varied losses of streamflow volume.
evaporation in summer season (3rd *L*-moment)	high-flow frequency	Extreme evaporation promotes lower average flow levels.
evaporation in winter season (1st *L*-moment)	flood probability and severity; high-flow frequency; baseflow	Regions with higher evaporation will have significantly reduced runoff because of the drop in water availability. Lower evaporation rates are also indicative of wetter conditions.
evaporation in winter season (2nd *L*-moment)	flood probability and severity; baseflow average and seasonality	High evaporation variability suggests fluctuating evaporation rates (and, hence, sporadic cloud cover and rainfall), indicating varied streamflow volumes..
evaporation in winter season (3rd *L*-moment)	flood probability and severity; baseflow	Extreme evaporation promotes lower average flow levels.
MSLP in summer season (1st *L*-moment)	flood probability and severity, baseflow average and seasonality	Low MSLP is often associated with monsoonal or cyclonic activity, when extreme floods become far more probable.
MSLP in summer season (2nd L-moment)	flood probability and severity; high-flow frequency; baseflow average and seasonality	Varied MSLP levels suggest a frequent passage of storm fronts, supporting a greater number of flow events and also promoting elevated baseflow.
MSLP in summer season (3rd *L*-moment)	flood severity; high-flow frequency	A more (mostly negatively) skewed MSLP distribution indicates a greater propensity for severe weather events, thus encouraging extreme streamflow.
MSLP in winter season (1st *L*-moment)	flood severity; high-flow frequency; baseflow average and seasonality	Reduced MSLP suggests the presence of a rain-bearing low or trough, promoting high-flow events.
MSLP in winter season (2nd *L*-moment)	all: flood probability and severity; high-flow frequency; baseflow	Varied MSLP levels suggest a frequent passage of storm fronts, supporting a greater number of flow events and also promoting elevated baseflow.
MSLP in winter season (3rd L-moment)	flood probability and severity; high-flow frequency; baseflow	Higher values suggest a greater inclination for fewer rain days, promoting intermittent or ephemeral stream behaviour and lower baseflow.

Out of the forty catchment descriptors, upstream area and channel skewness were the only attributes not significantly correlated with one of the six surface hydrology PCs at the more stringent Šidák correction factor (0.0013) when the full dataset was investigated. Nevertheless, with p-values of 0.021 (channel skewness vs PC4) and 0.0016 (upstream area vs PC6), significant connections were still evident at more traditional cut-off levels. Further,

upstream area is significantly correlated with four PCs (at the Šidák correction level) when non-perennial waterways are removed. Streams in upper catchments have a greater tendency to be non-perennial and their exclusions leads to greater prevalence of higher-order streams in relative terms. Consequently, upstream area becomes more pertinent.

The link between channel skewness and PC4 is mainly attributable to the variable's correlation with the average number of flow peaks in a year (p-value = 0.013). This link between channel skewness and annual number of flow peaks may partially be of an indirect nature, because both features are significantly related to topographical attributes pertaining to stream length (e.g. average flow length) and elevation (e.g. median elevation). Catchments with lower vertical relief or shorter stream lengths have a greater tendency for higher channel skewness. Higher channel skewness – synonymous with a more asymmetrical drainage pattern – results in less efficient flows into streams in some areas, thus impacting on local flow conditions. Hence, the inverse relationship between channel skewness and PC4 suggests a greater propensity for more frequent flow peaks when channel skewness is low.

The statistical findings are subsequently discussed separately for each PC.

4.1 Extreme flow severity

Higher mean daily rainfall (1st *L*-moment), rainfall variability and summer rain percentage are all strongly linked to extreme streamflow (represented by PC1; Figure 8a). Conversely, the number of rain days per year is negatively correlated with the occurrence of extreme flood events, with more rain days less likely to result in extreme flood events. Subcatchments with low numbers of rainy days per year tend to be associated with high mean daily rainfall (1st *L*-moment) and, therefore, higher probability of extreme flow events. The positive relationship between seasonal mean daily evaporation (1st *L*-moment) and PC1 is expected, because evaporation is negatively related to the number of rain days (rain-free days have a greater propensity for cloud-free conditions and increased evaporation). The negative association of mean MSLP conditions (1st *L*-moment) with PC1 indicates the importance of low-pressure

systems and the consequential enhancement of rainfall associated with these weather patterns (e.g. tropical lows, east coast lows and troughs). The relevance of mean summer MSLP is also reflected by its high TPE for PC1 (0.916_{AIC}; Figure A.2).

Figure 8

Variability of subsurface permeability and LSV, along with average LSV, are the non-climatic metrics with the strongest association with PC1. The 6_{max}-predictor regression model test identified subsurface permeability variability as the index with the highest TPE (0.999). This attribute is negatively correlated with PC1, suggesting that greater variability in subsurface property permits a greater proportion of runoff to infiltrate underground, potentially reducing the severity of extreme flow events.

Only one topographical trait (main stream slope) exhibits a correlation significant at the Šidák correction level (p-value < 0.0013; Table A.3). However, several additional topographical descriptors relating to elevation (longest flow path slope, maximum elevation, vertical range and average slope) have p-values below 0.01. All five topographical indices are positively correlated with the annual number of rain days, whereas the three slope attributes have a negative relation to mean daily rainfall. Consequently, the negative correlation between these topographical variables and PC1 is partially attributable to the propensity for more frequent, light rainfall events (e.g. drizzly conditions) in elevated terrain compared with areas closer to sea level. In addition, a significant proportion of the strong relationships will stem from the applied method: Basins with stream orders greater than five were further subdivided into subcatchments (Figure 3). Thus, upper subcatchments will generally be characterised by higher topography, steeper slopes and usually also more varied elevation – in contrast to the lower subcatchments that will mostly typify a more uniform, low-relief landscape. Because upstream flows will ultimately accumulate and reach the lower subcatchment, higher flow

volumes are expected in the latter, hence producing a negative relationship with topographical elevation, variability and gradient.

4.2 Extreme flow event probability and baseflow properties

PC2 embodies both the probability of extreme flow events (*L*-moments 3 to 5) and, to a lesser degree, baseflow attributes. When streamflow is highly variable (as reflected by larger values for *L*-moments 3-5), baseflow yield tends to be lower, particularly during summer.

Comparable to PC1, PC2 is most strongly linked to climate indices (Figure 7). Consequently, most of the climatic description for PC1 (section 3.1) also applies to PC2. However, contrary to PC1, *L*-moments 3 and 4 of daily rainfall both exhibit significant, positively correlated relationships with PC2. This result is not unexpected when the robust link between rainfall and runoff is considered, with PC2, to a large extent, defined by streamflow *L*-moments 3 to 5. Greater positive skewness and kurtosis both indicate heavier, more pronounced tails, translating to a greater prominence of days with extreme rainfall and elevated streamflow.

The strong correlation between percent summer rainfall (November – April) and average daily flow describes non-perennial watercourses in areas with highly seasonal rainfall. Further, more extreme rainfall tends to be experienced in regions with predominant summer rainfall, a pattern confirmed by the correlation analysis. Consequently, a concomitant increase in potential extreme flows is expected (Figure 8b).

To an even greater extent than for PC1, topographical descriptor main stream slope is also significantly connected to PC2, in addition to longest flow path slope, mean slope and elevation variability. Low vertical relief (general absence of steep slopes and dominance of flood plains), particularly if in conjunction with large area in steeper upstream subcatchments, can result in water backing up or flows slowing, especially when constriction points are present. Consequently, streamflow levels tend to be elevated for extended periods in areas of poor drainage, leading to a larger proportion of days with elevated flows (i.e. more highly skewed flow patterns).

Among non-climate variables, LSV has the strongest connection with PC2 (p-value < 0.0013; Table A.3). High LSVs (particularly in conjunction with low subsurface permeability) denote a larger proportion of rainfall converting to runoff because of low infiltration rates. Hence, LSV is strongly associated with extreme flow probability.

PC2 also strongly represents BFI (the higher the PC2 value, the lower the expected BFI). BFI has a strong negative association with evaporation, whereas regular rainfall (higher number of annual rain days) promotes baseflow by increasing soil saturation. In addition, steeper topography facilitates soil water drainage, encouraging elevated baseflow in these areas (Price, 2011).

Hale and McDonnell (2016) have specifically linked subsurface permeability to longer mean transit time of baseflow, buffering the river system to rainfall variability. Here, we have found that subsurface permeability and its extent of spatial uniformity are negatively linked to mean seasonal and long-term BFI. Thus, greater subsurface permeability and heterogeneity thereof are suggested to result in reduced baseflow, potentially a reaction to increased infiltration to deeper groundwater systems. The correlation results for non-perennial streams confirmed the negative relationship between mean BFIs and subsurface permeability, whereas the link with variability of subsurface permeability was less conclusive.

4.3 Low flow conditions

A relatively small number of catchment variables is significantly linked to PC3 (low flow represented by flow minima) based on the Šidák correction level (Figure 7), although the number increases more than threefold when the more lenient threshold level is applied (α = 0.05, Table A.3).

In contrast to the preceding PCs, climate variables have a subordinate role in determining PC3 values and, accordingly, minimum flow levels, although the number of annual rain days is important (as also evidenced by its incorporation into the BRMs; Figure 8d). PC3 has the strongest connection with bifurcation ratio, with its link to HDD also significant at the Šidák

correction factor (0.0013). Higher values for these morphometric parameters suggest a shorter time for the discharge to exit the catchment. Although this can amplify flood risk by increasing peak discharge, streamflow can also more quickly return to low levels after high-flow events, thus encouraging lower flow minima and explaining the inverse relationship between bifurcation ratios and PC3. Previous studies in mountainous regions of Puerto Rico (Garcia-Martinó et al., 1996) and the south-eastern Unites States (Price et al., 2011) have also highlighted HDD as a key predictor of low-flow behaviour, with a reverse association between low flow and HDD, in agreement with our findings. However, contrary to our result, Price et al. (2011) have found a positive relationship between low flow and bifurcation ratio. The contrasting results can possibly be attributed to differences in low-flow definitions (low-flow threshold over a certain period vs absolute flow minimum), along with dissimilarities in study scale and location.

The connection with mean slope is more complex. Although steeper slopes encourage rapid runoff (thus permitting a more rapid reversion to low flows), these regions are also commonly associated with a greater number of rainfall days per annum. Such rainy conditions are not conducive to low flow minima, ascribed to the positive relationship between mean slope and PC3 (low flow conditions).

The relatively poor performance of the PC3 regression models – and low number of predictors that are significantly correlated with this PC – can at least partially be ascribed to the large number of non-perennial streams (i.e. minimum streamflow values of 0 m^3/s) in Australia. Of the 750 gauges used for this analysis, 76.7% are situated in sites of intermittent or ephemeral flow. The diverse catchment properties of these non-perennial settings result in overall poorer performance of the statistical tests. When the correlation analysis is repeated by omitting the non-perennial streams, upstream area and mean MSLP in winter (in addition to bifurcation ratio and HDD) exhibit a significantly positive relationship with PC3 (p-value < 0.0013) and, thus, low-flow conditions, even though the statistical power is reduced by the smaller dataset (n = 175). Larger catchment areas will permit greater accumulation of

flows, thus increasing the minimum runoff volume. Conversely, lower mean MSLPs suggest a higher propensity for rainfall in the cooler months, thus producing runoff during a period when a large proportion of Australia receives limited precipitation. Upstream area and bifurcation ratio are also among the indices incorporated into the reduced (perennial-only) BRMs, with the R^2_{adj} for AIC (BIC) augmenting from 0.167 (0.122) to 0.344 (0.334). In addition, whereas the BIC model size remained unchanged (four, with upstream area substituting annual number of rain days), the AIC model decreased from 28 to 6, thus reducing likely overparameterisation.

4.3.1 The problematic case of ephemeral waterways

A large proportion of Australian streams is non-perennial in nature. Some of these watercourses are classified as intermittent, their seasonal flows sustained longer by groundwater supply. Ephemeral sites, however, are only recording flows for a brief duration (e.g. a few days) – immediately following significant precipitation. These extended periods of zero-flow have substantial impacts on a range of attributes. Specifically, the rainfall-runoff relationship can be altered considerably by antecedent conditions. Dry spells produce crusting of soils via chemical processes, hampering water infiltration in the absence of gentle pre-wetting – and enhancing erosion and flood risk. Surface crusting can also be produced by clay deposition after a significant flow event. Further, Zhang et al. (2017) highlighted that the Lyne-Hollick method, applied here, is not recommended for ephemeral streams because of the brief flow periods and prolonged absence of a slow flow component. Thus, when more reliable estimates are required for ephemeral systems, alternative baseflow derivation methods should be considered.

4.4 High-flow frequency

High-flow events (related to PC4) are defined as any periods when streamflow surpassed the 80th percentile at that site. The frequency of high-flow events is predominantly dictated by the annual number of rain days, as also evidenced by the negative relationship between PC4

and mean evaporation in both seasons (Figure 8c). Topography also greatly impacts on the high-flow recurrence interval because of the tendency for orographic enhancement of precipitation at higher altitudes. Catchments with higher and more varied elevation are predisposed to a greater number of high-flow events, aided by the faster passage of the runoff. This view is supported by the strong association between PC4 and HDD (positive) and flow distance (negative). HDD is a measure of how effectively runoff travels within a catchment. All these connections suggest short-duration high-flow events that occur more regularly in drainage basins with high PC4 values. Extreme runoff events are prone to be more significant (in terms of speed and instantaneous volume) in catchments with a greater capacity to transmit water, although the flow events also tend to be of shorter duration.

Although the LSV metrics are not significantly correlated with PC4, they are both incorporated into the BRMs. In addition, the 6_{max}-predictor regression models attributed the highest TPE, among non-climatic indicators, to the variability of LSV (0.742_{BIC}). When the regression analysis was repeated with non-perennial streams removed (n = 175; Table A.5), the AIC (BIC) R^2_{adj} for the BRMs improved from 0.452 (0.423) to 0.667 (0.551) despite the reduction in statistical power and a decrease in model size from 29 (15) to 26 (7). The non-perennial regression models incorporated mean LSV (inverse relationship) and variability of subsurface permeability (direct) regardless of whether the AIC or BIC was applied as the criterion, with mean LSV scoring a TPE of 0.432_{BIC}.

Lower LSVs and their variability (enhanced water infiltration or chance thereof) correspond to higher PC4 and greater number of flow peaks. This connection can be explained by water infiltration and, consequently, a more rapid reduction in streamflow. This permits water levels to drop below the 80th percentile faster and, thus, the potential for a new flow peak to arise.

4.5 Seasonal baseflow difference

PC5 summarises the seasonal BFI difference, represented by the ratio of the long-term winter to summer BFI values. Climate predictors dominate variables significantly associated with

baseflow seasonality (Figure 8f). Among these predictors, the 3rd L-moment of winter season evaporation is the most prominent index based on the strongest (inverse) correlation and highest TPE (0.837_{BIC}). The more extreme (right-skewed) the distribution of evaporation, the lower PC5 (ratio of summer over winter mean BFI). Evaporation reduces streamflow volume. Consequently, a more right-skewed evaporation pattern during the cooler months is expected to reduce winter baseflow yields, thus increasing the winter/summer BFI ratio. Variability of subsurface permeability has the second highest TPE (0.441_{BIC}) for PC5, whereas elevation-related attributes have the most significant (inverse) correlations among the non-climatic predictors. Because subsurface permeability is inversely linked to elevation attributes, a more variable permeability in headwater subcatchments encourages localised water infiltration where surface flow would otherwise be more dominant. Further, rainfall in Australian catchments tends to be summer-dominant. Hence, the proportion of runoff diverting to baseflow is expected to be greater in the winter period at most sites that permit water infiltration, thus potentially increasing the BFI ratio.

Previous studies indicate that watersheds at higher altitudes tend to produce greater baseflow yields (e.g. Rumsey et al., 2015). These results are confirmed here, with the altitude parameters positively correlated with seasonal and overall mean BFI. Conversely, elevation-related predictors are inversely linked to the winter/summer BFI ratio. The PC5 connection is stronger with summer than winter baseflow levels. Therefore, the derived negative relationship with the winter/summer BFI ratio is attributable to a more enhanced increase in mean summer baseflow with height (relative to winter conditions), thus reducing the ratio.

When the correlation and BRM were repeated with the perennial watercourses (n = 175; Table A.5), PC5 showed the most striking improvement in predictive strength, the AIC (BIC) results increasing from 0.143 (0.127) to 0.542 (0.516) despite model sizes remaining nearly constant, changing from 12 (4) to 11 (4). For these additional models, upstream area and proportion of summer rain are important, whereas elevation attributes were not significantly related. These differences can be explained by several aspects. Firstly, the full dataset of

750 gauges is much more disparate, encompassing a greater diversity in terms of climate and coastal proximity, making the derivation of a high-performing predictive model more challenging. Conversely, perennial streams are mostly limited to sites that are relatively near-coastal – including ranges feeding these coastal catchments – and typified by wet conditions (Figure 1). These regions include southeast Australia and, to a lesser extent, the wet tropics and southwest Australia. Secondly, lower-order streams have a greater tendency to be non-perennial and a comparatively large proportion of gauges in upper watersheds were thus excluded from the perennial subset. With higher-order waterways more prevalent in relative terms, upstream area becomes more relevant. And because the remaining sites are less diverse, the predictive power of the BRMs improved.

4.6 Baseflow

PC6 relates to winter baseflow and, to a lesser degree, long-term and summer BFI characteristics. The annual number of rain days has the weakest correlation with PC6 (p-value = 0.730). Yet, this predictor has the highest TPE (0.989) and is also incorporated into both the AIC and BIC BRMs. In addition, the correlation does become significant at the Šidák correction level (p-value < 0.0013) when non-perennial streams are removed.

Although atmospheric characteristics are important, the influence of topography and surface condition is more pronounced when streamflow is not extremely high. During extreme precipitation events, most rainfall will convert to runoff because of fully saturated soils, regardless of topography, whereas the catchment response will be more nuanced for less intense rainfall events. Variables that describe elevation are the most influential topographical features, with slope-related traits also significantly linked to PC6 and baseflow (Figure 8e). While some of these indices are also strongly connected to PC2, their relationship is reversed. BFI variability is positively related to these predictors. As baseflow attributes are incorporated into PC6 with a positive trend, and reversely with PC2, the connection of the elevation and slope descriptors and PC6 changed accordingly.

Various catchment properties were previously linked to baseflow. For instance, Post and Jakeman (1996) related baseflow recession in Victoria with catchment shape and slope, confirming our result. Conversely, Lacey and Grayson (1998) determined that the BFI is independent of topographical features in Victoria, with baseflow more closely associated with geology and vegetation, two attributes not directly included in our investigation. However, mean subsurface permeability – an indirect representative of geology – exhibited significant, inverse correlation with PC6 (and BFI) regardless of whether non-perennial streams were excluded (Figure 7 and Figure A.3), substantiating the importance of geology.

4.7 Frequency distributions

The sensitivity of the *L*–moments method to climatic extremes in seasonally arid and monsoonal zones is uncertain. In the seasonally arid tropics, many of the daily rainfall and streamflow values are zero, with intense rainfall maxima often occurring after prolonged dry periods. The recorded values will have significant influence on the 3rd and 4th *L*–moments and kurtosis, but the influences of these factors on the 5th *L*–moment (super-skewness) needs more research. The 5th *L*–moment is predicted to reliably determine flood parameters (e.g. river level and flow velocity in situations when extreme flood peaks over base flow are observed).

The method of *L*–moments is intrinsically related to the fundamental underlying frequency distribution that is used to describe the data. In Australia, a log-Pearson III (LP3) distribution was previously favoured to determine the frequency of intense rainfall events and is still widely used for Australian catchment studies (e.g. flood frequency analysis; Ball et al., 2019). The low probability (extreme rainfall) events are represented in the right-hand tail of these distributions and the nature of the tail varies between distributions. The generalised extreme value (GEV) distribution, fitted using *L*-moments, is now the recommended method to perform frequency analysis for rainfall in most circumstances (Ball et al., 2019). Ball et al. (2019) also declared, however, that neither GEV nor LP3 may adequately embody rainfall patterns in regions affected by tropical cyclones (TCs). The goodness of fit of the right-hand portion of

the distribution (and in some circumstances, the left-hand portion of the distribution) may significantly influence the probability values obtained, and the positions of the *L*–moments for the distribution. Consequently, if flood frequency is to be added to flood heights and velocity, then research is necessary into the underlying distributions that best describe the Australian rainfall data. Because of the large size and disparate nature of the Australian landmass – and varied climate – no frequency distribution is expected to consistently perform best throughout the continent. Yet, regional adjustments of frequency distribution for national-scale studies are not necessarily recommended because of the difficulty in defining adequate similarity criteria for grouping catchments (and climatic zones) and the potential for reduced reproducibility of the scientific results.

5 Conclusions

A variety of variables were examined to distinguish catchment types within Australia that may influence runoff regimes. A diverse dataset, sourced from varied government agencies or sub-agencies, was collated for this project to derive forty catchment characteristics from the themes of climate, topography, surface condition (Table 5). Their links to streamflow behaviour (represented by twenty descriptors summarised by six PCs) in Australian drainage basins was scrutinised. Archive inconsistencies between agencies and states required numerical assessment and standardisation before analysis. Data collation aimed to provide a consistent and robust framework for the interpretation of catchments within Australia. The lack of geographically consistent, long-term rainfall and river runoff records throughout Australia required methods that accommodate inconsistencies in the datasets while still producing reliable and reproducible results.

The correlation and regression analyses confirmed that climate variables tend to dictate streamflow behaviour, especially during high-flow periods. This outcome is in agreement with earlier studies that attributed a relatively small role to other index types such as soils and

geological attributes (Beck et al., 2015). During low-flow, however, intrinsic catchment properties like upstream area, bifurcation ratio, and average topographical slope within the catchment and along the main waterway become important (Smakhtin, 2001).

Further investigations are required to define the relative roles of the climatic and geomorphological drivers, particularly in subcatchments where they significantly interact. Both factors ultimately control the frequency and severity of flood response across the Australian continent. A degree of uncertainty in clarifying the relative influence of these factors comes from limitations in data availability, because a large proportion of drainage basins remain ungauged. In addition, some catchment parameters, such as antecedent soil moisture and temporal aspects of water table data, were recognised as important, but their dynamic spatial and temporal variability disqualified their inclusion in this study. These dynamic catchment attributes pertain to individual events with large spatial or temporal variability (e.g. storm type and duration) and are highlighted as an area of future focus to refine flood studies.

The difference in results – depending on whether non-perennial waterways are incorporated – illustrates that streamflow response to climatic and in situ properties is regionally highly varied. Thus, grouping of similar streams is recommended to create tailored regional models for stronger predictive performance. This notion was also discussed by Trancoso et al. (2017) who found regional- and scale-dependent connections between streamflow and catchment properties.

Several caveats are associated with this study. Only linearity was considered (except for the logarithmic transformation of some variables) when exploring the connection between catchment characteristics and streamflow properties. However, some catchment descriptors are likely linked to streamflow in a non-linear fashion, providing avenues for further research. The extreme seasonality of climate and, accordingly, streamflow is also problematic. A large proportion (76.7%) of the examined streamflow gauges are situated in non-perennial waterways. Many of these watercourses are classified as ephemeral. Such sites typically flow

only for brief periods and are thus typified by extended dry periods. In the absence of a sustained slow flow component, Zhang et al. (2017) highlighted that the Lyne-Hollick method is not recommended for ephemeral streams. Further, soil crusting is a common occurrence during prolonged dry periods, affecting surface permeability and, therefore, infiltration rates. In the absence of gentle pre-wetting prior to a significant rainfall event, these soil crusts enhance surface runoff, ultimately elevating flood risk. While these changes can be observed on a seasonal scale, Australia is also notorious for its interannual climate extremes (Jaffrés et al., 2018) and extended (multi-annual) periods of wet or drought conditions (Taschetto et al., 2016). This variability further complicates estimations of streamflow and groundwater recharge, thus also hampering management of water resources. A further issue is the biased data distribution, with the arid interior and tropical north underrepresented by the network of stream gauges. In addition, temporal records tend to be relatively brief, hampering the capture of extreme events with low recurrence rate. As data availability for exogenous factors, like rainfall, and intrinsic basin properties is more extensive, their association with streamflow properties can be utilised to infer catchment response to various flow scenarios.

The study outcomes represent amalgamation, interpretation and summary of a large number of environmental descriptors that influence, drive and interact with the distribution of water across the Australian landscape. The parameters chosen for statistical analysis resulted from a multidisciplinary approach to statistical methods, combined with expert understanding of climatic, geomorphic and hydrological systems to best interpret the results. The strong connection between catchment properties and streamflow characteristics provide opportunity for regionalisation in the absence of a dense stream gauge network that leaves most subcatchments essentially ungauged.

Acknowledgements

Streamflow data were downloaded from the Bureau of Meteorology (BoM) Water Data Online website. Rainfall station data were accessed from BoM's Climate Data Online website. Evaporation and mean sea level pressure data were supplied separately by the BoM. Permeability data were obtained from Geofabric. Catchment boundaries were derived from Geoscience Australia. Land use data were accessed from the Australian Department of Agriculture, Water and the Environment and soil data originated from CSIRO's Digital Atlas of Australian Soils. This study was financially supported by Suncorp Insurance. The authors gratefully thank the two anonymous reviewers for their valuable comments and suggestions.

Appendices A and B. Supplementary data

Supplementary data to this article can be found online.

References

Ashton, L.J. and McKenzie, N.J., 2001. Conversion of the Atlas of Australian Soils to the Australian Soil Classification, CSIRO Land and Water (unpublished).

Australian Soil Club. http://www.soil.org.au, accessed 7 March 2016.

Ball, J., Babister, M., Nathan, R., Weeks, W., Weinmann, E., Retallick, M. and Testoni, I., 2019. Australian Rainfall and Runoff: A guide to flood estimation. © Commonwealth of Australia (Geoscience Australia).

Beck, H.E., Roo, A.d. and Dijk, A.I.J.M.v., 2015. Global maps of streamflow characteristics based on observations from several thousand catchments. Journal of Hydrometeorology, 16(4): 1478-1501.

Brown, R.E., Graszkiewicz, Z., Hill, P.I., Neal, B.P. and Nathan, R.J., 2011. Predicting baseflow contributions to design flood events in Australia. In: E.M. Valentine, C.J. Apelt, J. Ball, H. Chanson, R. Cox, R. Ettema, G. Kuczera, M. Lambert, B.W. Melville and J.E. Sargison (Editors), Proceedings of the 34th World Congress of the International Association for Hydro-

Environment Research and Engineering: 33rd Hydrology and Water Resources Symposium and 10th Conference on Hydraulics in Water Engineering. Engineers Australia, Barton, A.C.T., pp. 64-73.

Busch, M.H., Costigan, K.H., Fritz, K.M., Datry, T., Krabbenhoft, C.A., Hammond, J.C., Zimmer, M., Olden, J.D., Burrows, R.M., Dodds, W.K., Boersma, K.S., Shanafield, M., Kampf, S.K., Mims, M.C., Bogan, M.T., Ward, A.S., Perez Rocha, M., Godsey, S., Allen, G.H., Blaszczak, J.R., Jones, C.N. and Allen, D.C., 2020. What's in a name? Patterns, trends, and suggestions for defining non-perennial rivers and streams. Water, 12(7): 1980.

Calver, A., 2001. Riverbed permeabilities: Information from pooled data. Groundwater, 39(4): 546-553.

Carlier, C., Wirth, S.B., Cochand, F., Hunkeler, D. and Brunner, P., 2018. Geology controls streamflow dynamics. Journal of Hydrology, 566: 756-769.

Castellarin, A., Kohnová, S., Gaál, L., Fleig, A., Salinas, J.L., Toumazis, A., Kjeldsen, T.R. and Macdonald, N., 2012. Review of applied-statistical methods for flood-frequency analysis in Europe. 978-1-906698-32-4, European Cooperation in Science and Technology (COST), 122 pp.

Charman, P.E.V., 1978. Soils of New South Wales: their characterization, classification, and conservation. Soil Conservation. Soil Conservation Service - Technical Handbook No. 1, New South Wales.

CSIRO and SKM, 2010. Baseflow assessment for the Murray-Darling Basin, CSIRO: Water for a Healthy Country National Research Flagship, 78 pp.

Dixon, H., Hannaford, J. and Fry, M.J., 2013. The effective management of national hydrometric data: experiences from the United Kingdom. Hydrological Sciences Journal, 58(7): 1383-1399.

Dürr, H.H., Meybeck, M. and Dürr, S.H., 2005. Lithologic composition of the Earth's continental surfaces derived from a new digital map emphasizing riverine material transfer. Global Biogeochemical Cycles, 19(4): GB4S10.

Erskine, W., Saynor, M. and Lowry, J., 2017. Application of a new river classification scheme to Australia's tropical rivers. Singapore Journal of Tropical Geography, 38(2): 167-184.

Garcia-Martinó, A.R., Scatena, F.N., Warner, G.S. and Civco, D.L., 1996. Statistical low flow estimation using GIS analysis in humid montane regions in Puerto Rico. JAWRA Journal of the American Water Resources Association, 32(6): 1259-1271.

Geoscience Australia, 1997. Australia's river basins 1997, Bioregional Assessment source dataset.

Geoscience Australia, 2006. GEODATA TOPO 250K Series 3 topographic data. Geoscience Australia, Canberra, ANZCW0703005458.

Geoscience Australia, 2011. Digital elevation model (DEM) - 3 Second Shuttle Radar Topography Mission (SRTM) derived hydrological digital elevation model (DEM-H) version 1.0, ANZCW0703014615.

Geoscience Australia, 2012. Surface Geology of Australia, 1:1 million scale dataset (2012 edition), ANZCW0703016455.

Gleeson, T., Smith, L., Moosdorf, N., Hartmann, J., Dürr, H.H., Manning, A.H., van Beek, L.P.H. and Jellinek, A.M., 2011. Mapping permeability over the surface of the Earth. Geophysical Research Letters, 38(2).

Hale, V.C. and McDonnell, J.J., 2016. Effect of bedrock permeability on stream base flow mean transit time scaling relations: 1. A multiscale catchment intercomparison. Water Resources Research, 52(2): 1358-1374.

Hartmann, J. and Moosdorf, N., 2012. The new global lithological map database GLiM: A representation of rock properties at the Earth surface. Geochemistry, Geophysics, Geosystems, 13(12).

Hill, P., Brown, R., Nathan, R. and Graszkiewicz, Z., 2013. Australian Rainfall and Runoff, Book 5, Chapter 4: Baseflow models. Institution of Engineers, Australia, Barton, ACT, pp. 21 (downloaded 1 August 2015).

Horton, R.E., 1945. Erosional development of streams and their drainage basins; hydrophysical approach to quantitative morphology. Geological Society of America Bulletin, 56(3): 275-370.

Hosking, J.R.M. and Wallis, J.R., 2005. Regional frequency analysis: an approach based on *L*-moments. Cambridge University Press.

Jaffrés, J.B.D., Cuff, C., Rasmussen, C. and Hesson, A.S., 2018. Teleconnection of atmospheric and oceanic climate anomalies with Australian weather patterns: a review of data availability. Earth-Science Reviews, 176: 117-146.

Karlsen, R.H., Bishop, K., Grabs, T., Ottosson-Löfvenius, M., Laudon, H. and Seibert, J., 2019. The role of landscape properties, storage and evapotranspiration on variability in streamflow recessions in a boreal catchment. Journal of Hydrology, 570: 315-328.

Kennard, M.J., Mackay, S.J., Pusey, B.J., Olden, J.D. and Marsh, N., 2010a. Quantifying uncertainty in estimation of hydrologic metrics for ecohydrological studies. River Research and Applications, 26(2): 137-156.

Kennard, M.J., Pusey, B.J., Olden, J.D., Mackay, S.J., Stein, J.L. and Marsh, N., 2010b. Classification of natural flow regimes in Australia to support environmental flow management. Freshwater Biology, 55(1): 171-193.

Kinkela, K. and Pearce, L.J., 2014. Assessment of baseflow seasonality and application to design flood events in southwest Western Australia. Australasian Journal of Water Resources, 18(1): 27-38.

Kuentz, A., Arheimer, B., Hundecha, Y. and Wagener, T., 2017. Understanding hydrologic variability across Europe through catchment classification. Hydrol. Earth Syst. Sci., 21(6): 2863-2879.

Lacey, G.C. and Grayson, R.B., 1998. Relating baseflow to catchment properties in south-eastern Australia. Journal of Hydrology, 204(1): 231-250.

Lyne, V. and Hollick, M., 1979. Stochastic time-variable rainfall-runoff modelling, Institute of Engineers Australia National Conference. Institute of Engineers Australia, Barton, Australia, pp. 89-92.

McKenzie, N., Jacquier, D., Isbell, R. and Brown, K., 2004. Australian soils and landscapes: an illustrated compendium. CSIRO Publishing, Melbourne, Australia, xv, 416 pp.

Merz, R. and Blöschl, G., 2005. Flood frequency regionalisation—spatial proximity vs. catchment attributes. Journal of Hydrology, 302(1–4): 283-306.

Meyboom, P., 1961. Estimating ground-water recharge from stream hydrographs. Journal of Geophysical Research, 66(4): 1203-1214.

Murphy, R., Graszkiewicz, Z., Hill, P., Neal, B. and Nathan, R., 2011. Australian Rainfall and Runoff revision project 7: Baseflow for catchment simulation, 205 pp.

Peña-Arancibia, J.L., van Dijk, A.I.J.M., Mulligan, M. and Bruijnzeel, L.A., 2010. The role of climatic and terrain attributes in estimating baseflow recession in tropical catchments. Hydrol. Earth Syst. Sci., 14(11): 2193-2205.

Post, D.A. and Jakeman, A.J., 1996. Relationships between catchment attributes and hydrological response characteristics in small Australian mountain ash catchments. Hydrological Processes, 10(6): 877-892.

Price, K., 2011. Effects of watershed topography, soils, land use, and climate on baseflow hydrology in humid regions: A review. Progress in Physical Geography, 35(4): 465-492.

Price, K., Jackson, C.R., Parker, A.J., Reitan, T., Dowd, J. and Cyterski, M., 2011. Effects of watershed land use and geomorphology on stream low flows during severe drought conditions in the southern Blue Ridge Mountains, Georgia and North Carolina, United States. Water Resources Research, 47(2).

Rahman, A., Haddad, K., Zaman, M., Ishak, E., Kuczera, G. and Weinmann, E., 2012. Australian rainfall and runoff revision projects, Project 5. Regional flood methods, 319 pp.

Rumsey, C.A., Miller, M.P., Susong, D.D., Tillman, F.D. and Anning, D.W., 2015. Regional scale estimates of baseflow and factors influencing baseflow in the Upper Colorado River Basin. Journal of Hydrology: Regional Studies, 4: 91-107.

Saft, M., Peel, M.C., Western, A.W. and Zhang, L., 2016. Predicting shifts in rainfall-runoff partitioning during multiyear drought: Roles of dry period and catchment characteristics. Water Resources Research, 52(12): 9290-9305.

Shanafield, M. and Cook, P.G., 2014. Transmission losses, infiltration and groundwater recharge through ephemeral and intermittent streambeds: A review of applied methods. Journal of Hydrology, 511: 518-529.

Singh, S.K., Pahlow, M., Booker, D.J., Shankar, U. and Chamorro, A., 2019. Towards baseflow index characterisation at national scale in New Zealand. Journal of Hydrology, 568: 646-657.

Smakhtin, V.U., 2001. Low flow hydrology: a review. Journal of Hydrology, 240(3): 147-186.

Snelder, T.H. and Biggs, B.J.F., 2002. Multiscale river environment classification for water resources management. Journal of the American Water Resources Association, 38(5): 1225-1239.

Snelder, T.H. and Booker, D.J., 2013. Natural flow regime classifications are sensitive to definition procedures. River Research and Applications, 29(7): 822-838.

Stein, J.L., Hutchinson, M.F., Pusey, B.J. and Kennard, M.J., 2009. Ecohydrological classification based on landscape and climate data. Appendix 8. In: B.J. Pusey, M.J. Kennard, J.L. Stein, J.D. Olden, S.J. Mackay, M.F. Hutchinson and F. Sheldon (Editors), Ecohydrological regionalisation of Australia: a tool for management and science. Innovations Project GRU36, Final Report to Land and Water Australia, pp. 56.

Su, C.-H., Costelloe, J.F., Peterson, T.J. and Western, A.W., 2016. On the structural limitations of recursive digital filters for base flow estimation. Water Resources Research, 52(6): 4745-4764.

Taschetto, A.S., Gupta, A.S., Ummenhofer, C.C. and England, M.H., 2016. Can Australian multiyear droughts and wet spells be generated in the absence of oceanic variability? Journal of Climate, 29(17): 6201-6221.

Trancoso, R., Phinn, S., McVicar, T.R., Larsen, J.R. and McAlpine, C.A., 2017. Regional variation in streamflow drivers across a continental climatic gradient. Ecohydrology, 10(3): e1816.

van Dijk, A.I.J.M., 2010. Climate and terrain factors explaining streamflow response and recession in Australian catchments. Hydrol. Earth Syst. Sci., 14(1): 159-169.

Veihmeyer, F.J. and Hendrickson, A.H., 1931. The moisture equivalent as a measure of the field capacity of soils. Soil Science, 32(3): 181-194.

Victorian Resources Online. http://vro.agriculture.vic.gov.au/dpi/vro/vrosite.nsf/pages/soil-home, accessed 7 March 2016.

Vidal-Abarca, M.R., Gómez, R., Sánchez-Montoya, M.M., Arce, M.I., Nicolás, N. and Suárez, M.L., 2020. Defining dry rivers as the most extreme type of non-perennial fluvial ecosystems. Sustainability, 12(17): 7202.

Villeneuve, S., Cook, P.G., Shanafield, M., Wood, C. and White, N., 2015. Groundwater recharge via infiltration through an ephemeral riverbed, central Australia. Journal of Arid Environments, 117: 47-58.

Wagener, T., Wheater, H.S. and Gupta, H.V., 2004. Rainfall-runoff modelling in gauged and ungauged catchments. Imperial College Press, London.

Zhang, J., Zhang, Y., Song, J. and Cheng, L., 2017. Evaluating relative merits of four baseflow separation methods in Eastern Australia. Journal of Hydrology, 549: 252-263.

Zhang, Y., Viney, N., Frost, A., Oke, A., Brooks, M., Chen, Y. and Campbell, N., 2013. Collation of Australian modeller's streamflow dataset for 780 unregulated Australian catchments, CSIRO, Australia, 115 pp.

Zimmer, M.A. and Gannon, J.P., 2018. Run-off processes from mountains to foothills: The role of soil stratigraphy and structure in influencing run-off characteristics across high to low relief landscapes. Hydrological Processes, 32(11): 1546-1560.

Figure Captions

Figure 1: Distribution of unregulated, WDO-derived stream gauges in Australia with a minimum data record of 15 years. The colour scheme distinguishes non-perennial and permanent streams. Borders of states and territories are also shown.

Figure 2: Spatial variations of a) long-term, b) summer and c) winter mean BFI, as well as d) the winter/summer BFI ratio.

Figure 3: Stepwise progression of the subcatchment delineation with CatchmentSIM. a) The National River Basin Boundary (NRBB) is used to clip the topography with a 10 km buffer to account for differences in border estimates between the two datasets. b) The Horton's stream orders are determined for the vector stream network within the NRBB. The 5th-order streams are then used to c) divide the basin into subcatchments, with the boundaries defined by the topography. Each segment of 6th- and higher-order streams is delineated as a separate subcatchment.

Figure 4: Distribution of weather stations with a minimum of a) 30 years of rainfall, and two years of b) evaporation and c) mean sea level pressure (MSLP) data. Rainfall stations are further grouped based on the number of years with near-complete (>350 days of) annual data.

Figure 5: Flow chart for the calculation of the soil code, field capacity score (FCS), land use score (LUS) and land surface value (LSV). Australian Soil Classification (ASC), depth of soil profile rank and textural class are derived from Ashton and McKenzie (2001).

Figure 6: Flow chart of the land surface value (LSV) determination method based on the field capacity score (FCS) and land use score (LUS).

Figure 7: Correlation coefficients between the surface hydrology PCs and individual catchment characteristics (n = 749). Bars extending beyond the dashed lines are statistically significant at the Šidák correction level (p-value < 0.0013).

Figure 8: Schematic diagrams of the relationship between streamflow and catchment descriptors.

Highlights

- Australian surface flow is compared to forty diverse catchment descriptors
- Climate and rainfall characteristics dominate Australian streamflow behaviour
- Topographical and surface conditions greatly influence low-flow properties
- Non-perennial streams affect infiltration capacity and proportional runoff
- Uniform application of methods is not always recommended, as catchments are diverse

Author Contributions

Jasmine B. D. Jaffrés: Conceptualisation, Methodology, Software, Validation, Formal analysis, Investigation, Writing - original draft, Writing - review & editing, Visualisation. **Ben Cuff**: Conceptualisation, Methodology, Software. **Chris Cuff**: Conceptualisation, Writing - review & editing, Supervision, Funding acquisition. **Iain Faichney**: Software. **Matthew Knott**: Conceptualisation, Supervision. **Cecily Rasmussen**: Conceptualisation, Writing - review & editing, Supervision, Funding acquisition.